Palaeomagnetic results from Palaeocene basalts from Mongolia reveal no inclination shallowing at 60 Ma in Central Asia

Fatim Hankard, Jean-Pascal Cogné, France Lagroix, Xavier Quidelleur, Vadim A. Kravchinsky, Amgalan Bayasgalan, Purevdorj Lkhagvadorj

Geophys. J. Int. (2008) **172,** 87–102 doi: 10.1111/j.1365-246X.2007.03619.x

Palaeomagnetic results from Palaeocene basalts from Mongolia reveal no inclination shallowing at 60 Ma in Central Asia

Fatim Hankard,[1] Jean-Pascal Cogné,[1] France Lagroix,[1] Xavier Quidelleur,[2] Vadim A. Kravchinsky,[1,*] Amgalan Bayasgalan[3] and Purevdorj Lkhagvadorj[3]

[1]*Laboratoire de Paléomagnétisme, Institut de Physique du Globe de Paris, Université Paris* 7, 4 *Place Jussieu,* 75252 *Paris Cedex* 05*, France. E-mail: hankard@ipgp.jussieu.fr*

[2]*Laboratoire de Géochronologie Multi-techniques U.P.S. – I.P.G.P., Bat.* 504*, Sciences de la Terre, Université Paris Sud,* 91405 *Orsay, France*

[3]*Mongolian University of Science and Technology,* PO Box 49/418*, Ulaanbaatar* 210349*, Mongolia*

Accepted 2007 September 11. Received 2007 August 20: in original form 2007 June 8

SUMMARY

We present the results of a palaeomagnetic study of 277 cores drilled at 35 sites, in 32 basaltic flows from three Early Palaeocene volcanic regions in the Gobi Desert, Mongolia, at Sumber Uul (62.2 Ma; 42.6°N/104.0°E), Tulga (62.0 Ma; 43.2°N/104.1°E) and Khuts Uul (57.1 Ma; 43.2°N/104.6°E) localities. Samples from Sumber Uul (62.2 ± 0.9 Ma) and Khuts Uul (57.1 ± 0.8 Ma) localities were dated using the K-Ar Cassignol–Gillot technique. Stepwise thermal and alternating field demagnetizations isolated a stable A component of magnetization carried by single domain (SD) to nearly SD magnetite. We interpret this A component to be the primary magnetization of these basaltic lava flows.The Sumber Uul and Tulga data were combined and recomputed at the Sumber Uul locality because of their similar ages. The palaeopoles computed from the A components lie at $\lambda = 85.2°$N, $\phi = 92.5°$E, dp/dm = 3.9/4.9 ($n = 14$ flows) for Sumber Uul-Tulga (average age: 62.1 ± 5.9 Ma) and $\lambda = 69.6°$N, $\phi = 148.0°$E, dp/dm = 6.3/7.3 ($n = 14$ flows) for Khuts Uul (average age: 57.1 ± 0.8 Ma). The palaeomagnetic inclinations are steeper than expected at the sites and consequently our palaeopoles occupy a near-sided position with respect to the 60 Ma reference apparent polar wander path (APWP) pole for Europe (Besse & Courtillot 2002). However, they appear to fully conform to the new high-resolution APWP poles for the 65–42 Ma period of Moreau *et al.* (2007). Following these authors, we interpret this anomalous near-sided position of our poles as arising from a rapid true polar wander (TPW) event in the Palaeocene, highlighted by a cusp at anomalies 26–25 (61–56 Ma), inexistent in the European APWP of Besse & Courtillot (2002). We conclude that our new data do not reveal any anomalous shallow inclinations in the Central Asia Palaeocene effusive rocks which is consistent with the Late Jurassic/Early Cretaceous age of Mongol-Okhotsk ocean closure and amalgamation of Amuria and Siberia, forming a rigid entity since then.

Key words: Palaeomagnetism applied to tectonics; Rock and mineral magnetism; Asia.

1 INTRODUCTION

Palaeomagnetic studies undertaken on Cretaceous and Tertiary red beds from the different Asian blocks repeatedly revealed anomalously shallow inclinations (Huang & Opdyke 1992; Chen *et al.* 1993a; Gilder *et al.* 1993; Westphal 1993; Thomas *et al.* 1994; Halim *et al.* 1998b) with respect to the inclinations which can be computed at a given locality using the reference apparent polar wander paths (APWP) of Europe (Besse & Courtillot 2002). For the Cretaceous period, these low palaeomagnetic inclinations have been interpreted as correlating with the ∼50 Ma India–Asia collision (Patriat & Achache 1984) and the ongoing penetration of the Indian plate into the Asian continent during the Tertiary (Molnar & Tapponnier 1975; Tapponnier & Molnar 1979; Patriat & Achache 1984). Thus, the Asian microblocks, located further south than expected from the European APWP, were translated northwards under the effect of the India–Asia collision (Enkin *et al.* 1992; Yang & Besse 1993; Chen *et al.* 1993b; Halim *et al.* 1998a, b). Recent studies however still debate on the amount of this northward movement (e.g. Gilder *et al.* 2003; Huang *et al.* 2005, 2006; Sun *et al.* 2006a, b). The picture grows more complicated when it comes to the Tertiary

*Now at: Physics Department, University of Alberta, Edmonton AB, Canada T6G 2J1.

data, for which the palaeomagnetic inclinations are also shallower than those deduced for Central Asia from the European reference APWP (Chen *et al.* 1993b; Halim *et al.* 1998b; Cogné *et al.* 1999; Sun *et al.* 2006b; Hankard *et al.* 2007a). However, the amount of intracontinental shortening between Central Asian mobile blocks (Tibet, Tarim, Qaidam, etc.) and northeastern stable blocks (e.g. Siberia, North and South China. . .) inferred from the anomalously shallow Cenozoic inclinations should be about twice the amount deduced from the Cretaceous data. Such quantities contradict geological observations and topographic constraints. Several possible causes have been proposed to explain these too shallow inclinations, amongst which syn-sedimentary or compaction-induced inclination shallowing, poor age control, tilted dipole, non-dipolar geomagnetic field geometry, tectonic shortening, poorly constrained APWP for Europe and non-rigidity of the Eurasian plate (Gilder *et al.* 1993; Thomas *et al.* 1993; Chauvin *et al.* 1996; Cogné *et al.* 1999; Si and Van der Voo 2001; Van der Voo and Torsvik 2001; Tauxe 2005; Yan *et al.* 2006; Hankard *et al.* 2007a).

Because most of the Cretaceous and Tertiary palaeomagnetic results from Central Asia were obtained on sedimentary rocks, sedimentary processes were naturally suspected to cause a large part of the observed palaeomagnetic inclination anomalies (Gilder *et al.* 2001, 2003; Tan *et al.* 2003; Liu *et al.* 2003; Yan *et al.* 2005, 2006; Narumoto *et al.* 2006). Nevertheless, Thomas *et al.* (1993) reported a significant difference between observed and expected inclination of $15^\circ \pm 7^\circ$ obtained from the Toru-Aygyr Eocene basalts in the Issyk-Kul basin (west Tien Shan). This value is similar to the one ($16^\circ \pm 5^\circ$) they obtained from sedimentary rocks. In addition, our recent palaeomagnetic results obtained from Tertiary igneous rocks from Mongolia (Hankard *et al.* 2007a), also revealed significant shallowing of $\sim 10^\circ$ ($8.0^\circ \pm 4.7^\circ$ at 40 Ma and $9.7^\circ \pm 3.3^\circ$ at 30 Ma) between observed palaeomagnetic inclination in igneous rocks and expected ones at 40 and 30 Ma. Therefore, no sedimentary processes could reasonably be invoked to explain these systematic discrepancies.

In order to unravel this complex inclination shallowing anomaly in Central Asia, we report new palaeomagnetic results and K-Ar geochronological dating from Early Palaeocene basalts collected from three localities in the southeastern Gobi Desert (Mongolia) during two field trips in 1999 and 2004 (Fig. 1). Our (Hankard *et al.* 2007b) and others (Zhao *et al.* 1990; Pruner 1992; Cogné *et al.* 2005) Cretaceous results from the Amuria block are concordant with the reference APWP poles for Europe while those at 40 and 30 Ma are not (Hankard *et al.* 2007a). The aim of this study is to fill this analytical gap between $\sim$100 and 40 Ma. Results from the Mongolian Palaeocene basalts should, therefore, shed light on the Inclination Anomaly in Asia. To this purpose, we have sampled Palaeocene effusive formations from the Sumber Uul (42.6°N, 104.0°E, Fig. 1), the Tulga (43.2°N, 104.1°E), and the Khuts Uul (43.2°N, 104.6°E) regions.

2 GEOLOGICAL SETTING AND FIELD SAMPLING

2.1 Sumber Uul (42.6°N, 104.0°E)

The Sumber Uul region (Fig. 1), is a large basaltic plateau that consists at least of 10 distinct lava flows. These flows lie on top of flat-lying red-coloured sediments. In this region, we sampled ten sites corresponding to ten distinct flows for a total of 80 cores. On average, eight cores were taken at each site, using a gasoline-powered drill, and were oriented *in situ* using magnetic and sun compasses in order to check and correct for local magnetic field declination. Both solar and magnetic readings were available for all samples. The average local magnetic declination computed after magnetic and sun azimuths measured in the field is $-1.0^\circ \pm 1.5^\circ$, consistent with the -2.0° declination computed after the International Geomagnetic Reference Field (IGRF) at Sumber Uul locality for the summer of 2004. We also collected two hand samples for geochronological dating at one site (135).

2.2 Tulga (43.2°N, 104.1°E)

The village of Tulga is located near Dzun-Saykhan Mountains, in the Gobi Desert (Fig. 1). This locality exposes seven distinct basaltic lava flows, which occasionally presents some weak dips. However, after our field observations, the underlying sediments that outcrop locally have horizontal bedding surfaces. We therefore, assume that Tulga flows are flat-lying, and that local weak dips are linked to emplacement rather than to tectonics. We sampled these flows at seven sites corresponding to each flow, totalling 53 cores. Cloudy weather resulted in both solar and magnetic readings being possible for only 26 of the 53 cores. The average local magnetic declination computed after magnetic and sun azimuths measured in the field is $1.2^\circ \pm 0.9^\circ$, rather consistent with the IGRF declination of -2.0° in the Tulga region. This area was sampled in the first field trip of 1999 during which we did not take hand samples for geochronology.

2.3 Khuts Uul (43.2°N, 104.6°E)

Khuts Uul is a volcanic mountainous region located $\sim$50 km south of the Dalandzadgad town, in the Gobi Desert (Fig. 1). In this area, basalt flows outcrop at either side of the Buurhin-Khjar river canyon. Ten sites for a total of 81 cores (sites 50–59 corresponding to nine distinct flows) were drilled north of the canyon where the thickness of individual flows locally exceeds 3 m. South of the canyon, eight sites for a total of 63 cores (sites 42–49 corresponding to six distinct flows were sampled. Flows occasionally overlie volcanoclastic sediments that present north and northeast weak tilts. The significance of these tilts is discussed in Section 4.3.4. Both solar and magnetic readings were possible for only 52 cores, and the differences averaged $-3.2^\circ \pm 1.1$. This value is consistent with the -2.2° IGRF declination. Two hand samples were taken from two sites (42 and 46) for geochronology.

3 GEOCHRONOLOGY

Age determinations of samples from Sumber Uul and Khuts Uul localities investigated in this study were done at the Geochronology Multitechniques U.P.S.-I.P.G.P. laboratory at the Université d'Orsay following the Cassignol–Gillot K-Ar technique (Cassignol & Gillot 1982). This method is based on a double isotopic comparison between atmospheric argon and argon extracted from the sample using a mass spectrometer identical to the one described by Gillot & Cornette (1986). The ^{40}Ar signal calibration is performed prior to each analysis using a 0.1 cm^3 air pipette calibrated by volumetric determination and by repeated analyses of an inter-laboratory standard GL-O with recommended value of 6.679×10^{14} at g^{-1} of ^{40}Ar* (Odin *et al.* 1982). Typical uncertainties of 1 per cent are reached for ^{40}Ar calibration and K content measurement. The detection limit of the system is 0.1 per cent of ^{40}Ar* (Quidelleur *et al.* 2001). Ages were calculated using the decay constants proposed by Steiger &

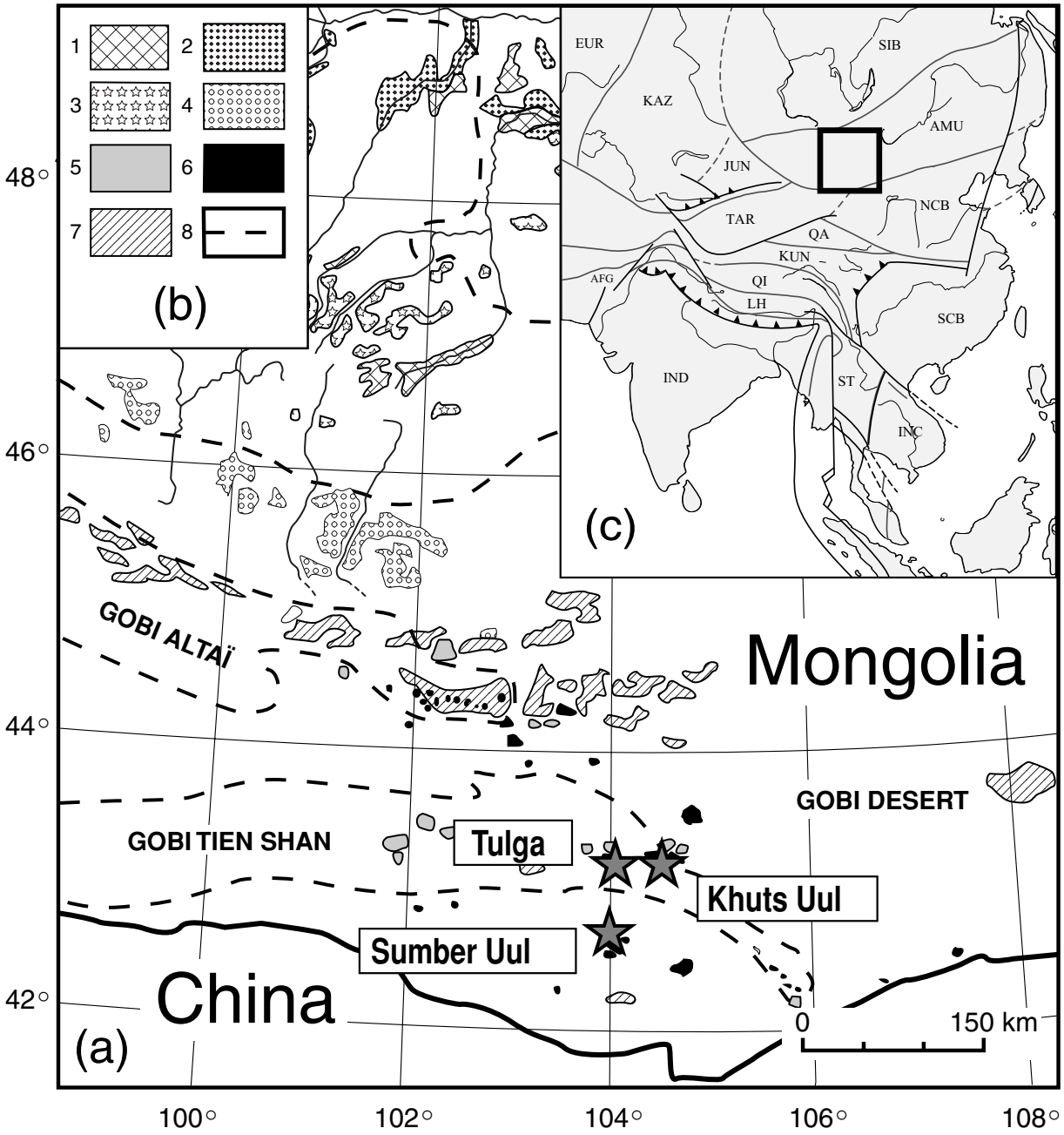

Figure 1. (a) Simplified map of Late Mesozoic–Cenozoic volcanic fields in Southern and Central Mongolia (after Kovalenko *et al.* 1997). Grey stars: Khuts Uul (57.1 ± 0.8 Ma), Tulga (62.0 ± 5.0 Ma), and Sumber Uul (62.2 ± 0.9 Ma) localities; (b) Legend: (1) Pleistocene–Holocene; (2) Pliocene; (3) Middle Miocene; (4) Late Oligocene and early Miocene; (5) Early Cenozoic; (6) Late Cretaceous; (7) Late Jurassic and Early Cretaceous and (8) Boundaries of highlands and ranges. (c) Inset: situation map of Fig. 1a in Asia, with main blocks indicated (AMU: Amuria, AFG: Afghanistan, EUR: Eurasia main plate, INC: Indochina, IND: India JUN: Junggar, KAZ: Khazakhstan, KUN: Kunlun, LH: Lhasa, MBT: Main Boundary Thrust, NCB: North China Block, QA: Qaidam, QI: Qiangtang, SCB: South China Block, SIB: Siberia, ST: Shantaï and TAR: Tarim).

Jaeger (1977). Analyses were duplicated and yielded concordant value at the 1σ level. The mean ages and uncertainties have been obtained by weighting each duplicate by their radiogenic content. The detailed procedure of sample preparation in the laboratory is described in Hankard *et al.* (2007b).

For the Sumber Uul locality, we have obtained a mean age of 62.1 ± 0.9 Ma. This age is younger than a previously published K-Ar age of 71 ± 4 Ma by Yarmolyuk *et al.* (1995). However, the accuracy and reliability of our own K-Ar ages using the Cassignol–Gillot technique (Cassignol & Gillot 1982) are underlined by the quasi-perfect reproducibility of two independent determinations of potassium as well as argon contents of the same sample. We thus prefer to rely on our new mean age of 62.1 ± 0.9 Ma for basalt flows from the Sumber Uul region.

Concerning the Tulga locality, we did not take any sample for dating during the 1999 field trip. We thus rely on the determinations of Yarmolyuk *et al.* (1995) and Shuvalov & Nikolaeva (1985) who reported an emplacement age of the outcropping basaltic flows

of 62.0 ± 5.0 and 61 Ma, respectively. These ages are consistent with one another. Furthermore, because of Tulga's proximity to the Sumber Uul locality (∼70 km) and their identical palaeomagnetic directions (see Section 4.3.3), we assume an emplacement age of 62.0 ± 5.0 Ma for the flows at Tulga.

According to Yarmolyuk *et al.* (1995), the Khuts Uul basalt flows yielded K-Ar ages ranging from 47.0 ± 3.0 to 73.0 ± 5.0 Ma. Our own K-Ar age determination, while falling within their 26 Myr window, provides a more precise age of 57.1 ± 0.8 Ma for the sampled Khuts Uul flows. This value agrees well with another previously published K-Ar age of 57.0 ± 5.0 Ma by Shuvalov & Nikolaeva (1985). We thus retain our new mean age of 57.1 ± 0.8 Ma for basalt flows from the Khuts Uul region.

4 PALAEOMAGNETIC AND ROCK MAGNETIC ANALYSES

4.1 Method

In the laboratory, the standard 2.5 cm-diameter cores drilled in the field were segmented into 2.2 cm-long specimens. Each core produced two to three specimens. All measurements were performed at the Institut de Physique du Globe de Paris (IPGP) in the palaeomagnetic research group's magnetically shielded room on the Jussieu campus or in the laboratories on the St Maur campus. Magnetic remanences were measured using an Agico JR5 or JR6 spinner magnetometer. Most specimens were thermally demagnetized, over 19 temperature steps up to 590–600 °C (sometimes 620 °C), in a nearly zero-field laboratory built furnace. Sample orientation was inverted about the *z*-axis which parallels the oven's axis, following each step, in order to detect any spurious magnetization that could have resulted from the small ∼10 nT residual magnetic field in the furnace. Alternating field (AF) demagnetization was performed on a limited number of samples over 14 steps up to 100 mT. Demagnetization results were plotted as orthogonal vectors diagrams (Zijderveld 1967) and also as equal-area projections. Palaeomagnetic directions were determined using either principal component analysis (Kirshvink 1980) or remagnetization great circles (Halls 1978). Site-mean directions were calculated using Fisher statistics (Fisher 1953), or using the statistics of McFadden & McElhinny (1988) for combined directional data and great circles. All palaeomagnetic data processing was carried out using the PalaeoMac software of Cogné (2003).

The magnetic mineralogy and carriers of the palaeomagnetic record were investigated on selected specimens found to be representative based on the palaeomagnetic analyses. Unblocking and blocking temperatures were determined from the temperature dependence of magnetic susceptibility curves measured on a Kappa-bridge KLY-3 equipped with a CS-3 furnace. Thermomagnetic experiments were conducted in air or argon. Hysteresis loops were measured using a laboratory-made translation inductometer in ±800 mT. Isothermal remanent magnetizations (IRM) were imparted, using the same instrument, up to 750 mT.

4.2 Rock magnetic results

The thermomagnetic susceptibility curves at all three localities display a fairly uniform behaviour. Unblocking and blocking temperatures (T_{UB} and T_B) determined from heating and cooling curves, respectively, following the graphical method (Grommé *et al.* 1969), are listed in Table 1. A histogram of T_{UB}, shown in Fig. 2, demonstrates that the dominant T_{UB} equals to or is very near the Curie temperature of stoichiometric magnetite (585 °C). Heating and cooling curves, in the vicinity of magnetite's unblocking/blocking temperature, are reversible (or nearly, average $\Delta T = 9$ °C) at Khuts Uul and Sumber Uul while in Tulga specimens magnetite's T_B is on average 34 °C lower than its T_{UB} probably related to the overall coarser magnetic grain size of Tulga samples (see below). Below ∼500 °C all samples display irreversibility, which is minimized in experiments conducted in argon.

Typical curves at all three localities are shown in Fig. 3. The heating induced alteration results in an overall decrease in bulk susceptibility upon returning to room temperature, ranging from 10 per cent to up to nearly 50 per cent, suggesting an oxidation reaction or mineral phase inversion to a lesser magnetic phase. The altered state of the specimens after a complete cycle is stable given that a repeat heating and cooling cycle produced perfectly reversible results retracing the original cooling curve (data not shown). On heating, susceptibility increases defining a broad maximum between 150 and 400 °C, absent in cooling curves. The general reversibility of the curves above 500 °C suggests that magnetite is not being oxidized. Therefore, a more likely scenario is the inversion of a mineral phase to a lesser magnetic phase, most likely pre-existing maghemite, resulting from the low temperature oxidation of magnetite to hematite. Thermal demagnetisations of NRM data support this interpretation and will be presented in Section 4.3.

IRM acquisition curves were measured on the four Sumber Uul specimens. Saturation is reached between 300 and 450 mT and mean acquisition fields range between 60 and 85 mT. These results, in addition to the thermomagnetic curves, support the dominance of magnetically soft minerals such as magnetite and maghemite.

Hysteresis loops are closed and saturated in fields between 300 and 400 mT, in agreement with IRM acquisition data. Furthermore, the average magnetic grain size can be determined from the hysteresis loop derived parameters. The Day plot for magnetite and titanomagnetite (Day *et al.* 1977; Dunlop 2002) shown in Fig. 4 indicates that the measured specimen cluster about two mean grain sizes. Sumber Uul and Khuts Uul specimens, with the exception of Khuts Uul specimens from flows 51 and 58, plot very near the theoretical uniaxial single domain (SD) magnetite particle lying in between the SD + multidomain (MD) and SD + superparamagnetic (SP) mixing curves of Dunlop (2002). Several thermomagnetic curves from these localities displayed Hopkinson peaks at temperatures just below T_{UB} and T_B (for example see specimen 135–497 in Fig. 3) attesting to the presence of SD particles near the SD/SP threshold. Tulga specimens and specimens from flows 51 and 58 at Khuts Uul show slightly coarser mean magnetic grain size falling on the SD + MD mixing curve near the 50 per cent SD to MD contribution mark (Dunlop 2002).

The presented rock magnetic data convincingly demonstrate that the palaeomagnetic record is principally carried by SD to nearly SD magnetite.

4.3 Palaeomagnetic results

4.3.1 Sumber Uul

We demagnetized 79 basalt specimens using stepwise thermal and alternating field (AF) demagnetization up to maximum temperature of 600 °C and peak AF field of 100 mT. Samples showed rather strong natural remanent magnetization (NRM) intensities, generally ranging from 1 to 10 A m^{-1}. However, a few samples show higher NRM intensities in the range of 10–30 A m^{-1} (as high as 87 A m^{-1}

Table 1. Rock magnetic parameters derived from hysteresis loops and measured from thermomagnetic curves of susceptibility (K) for selected specimens at all three localities.

		Hysteresis loop						Temperature dependance of K		
Id/flow	Specimen #	M_S (mAm^2 kg^{-1})	M_{RS} (mAm^2 kg^{-1})	M_{RS}/M_S	$\mu_o H_C$ (mT)	$\mu_o H_{CR}$ (mT)	H_{CR}/H_C	T_{UB} (°C)	T_B (°C)	
Sumber Uul										
134	488	801.0	265.0	0.3310	40.20	72.6	1.8	602	584	in air
135	497	832.0	302.0	0.3630	32.10	55.4	1.7	588	565	in air
137	517	982.0	381.0	0.3880	41.80	66.7	1.6	594	586	in air
140	537	780.0	311.0	0.3980	33.20	53.4	1.6	604	603	in air
Tulga										
35	280	1445.0	299.5	0.2072	24.66	51.4	2.1	580	544	in argon
36	288	1734.0	371.0	0.2137	23.97	48.3	2.0	572	536	in air
37	299	1083.0	205.8	0.1900	21.64	49.6	2.3	577	547	in argon
38	301	665.0	146.2	0.2178	26.02	58.5	2.2	600	576	in argon
39	315	1361.0	268.0	0.1969	28.65	63.0	2.2	581	529	in air
40	318	–	–	–	–	–	–	597	573	in argon
Khuts Uul										
43	343	–	–	–	–	–	–	566	530	in air
								317	284	
44	354	–	–	–	–	–	–	462	469	in air
								607	598	
45	361	–	–	–	–	–	–	–	351	in air
								601	597	
50	396	–	–	–	–	–	–	580	567	in air
51	405	800.0	179.4	0.2242	26.80	56.5	2.1	587	594	in air
52	416	–	–	–	–	–	–	591	591	in air
53	419	793.0	289.0	0.3640	25.69	49.8	1.9	∼420	∼375	in air
								604	604	
54	429	383.0	140.3	0.3660	32.10	61.1	1.9	584	585	in air
55	437	799.0	271.7	0.3400	33.60	61.8	1.8	591	582	in air
56	450	299.5	332.0	0.3790	38.60	67.0	1.7	586	575	in air
57	455	509.0	209.0	0.4110	41.20	72.0	1.7	589	589	in air
58	462	1137.0	206.6	0.1817	20.25	45.8	2.3	586	584	in air
59	474	–	–	–	–	–	–	598	591	in air

Id/Flow: Site or flow names; Specimen #: specimen number; M_s: Saturation magnetization, M_{RS}: Saturation remanent magnetization; H_c: Coercive force; H_{CR}: Remanent coercive force; T_{UB} (T_B): Unblocking (Blocking) temperature

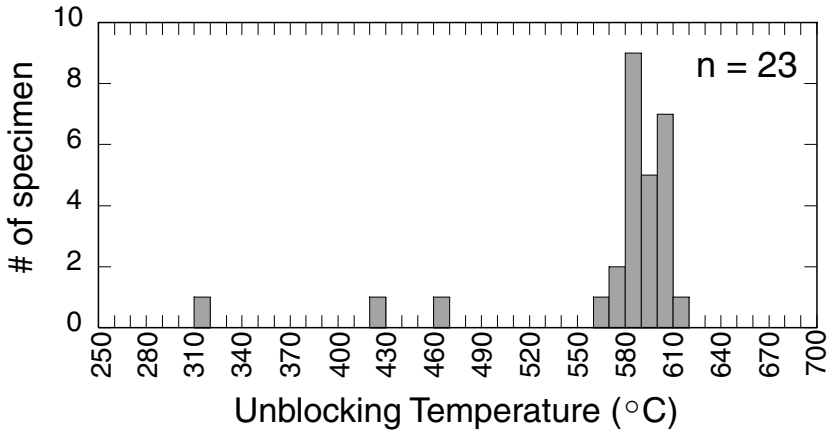

Figure 2. Histogram of unblocking temperatures of analysed specimens (Table 1) reveals that the dominant unblocking temperature equals or is near the Curie temperature of stoichiometric magnetite (585 °C).

in one specimen from site 131). These higher intensities which could be due to lightning are easily cleaned by peak fields around 30–40 mT or by heating to 200–300 °C.

Two typical examples of magnetization behaviour during thermal and AF demagnetization of samples from Sumber Uul are shown in Figs 5(a) and (b), and they illustrate the general behaviour of most samples. In sites 133, 134, 135 and 140, the demagnetization path linearly converges towards the origin of orthogonal plots (Fig. 5a) defining a single component of magnetization, hereafter referred to as component A. In the other sites (131, 132 and 136–139), a second component (component B) of either viscous or weathering origin unblocks by 200 °C or in peak field around 4 mT. In some specimens, the magnetization path linearly trends towards the origin of the diagram after removal of component B, thus defining a

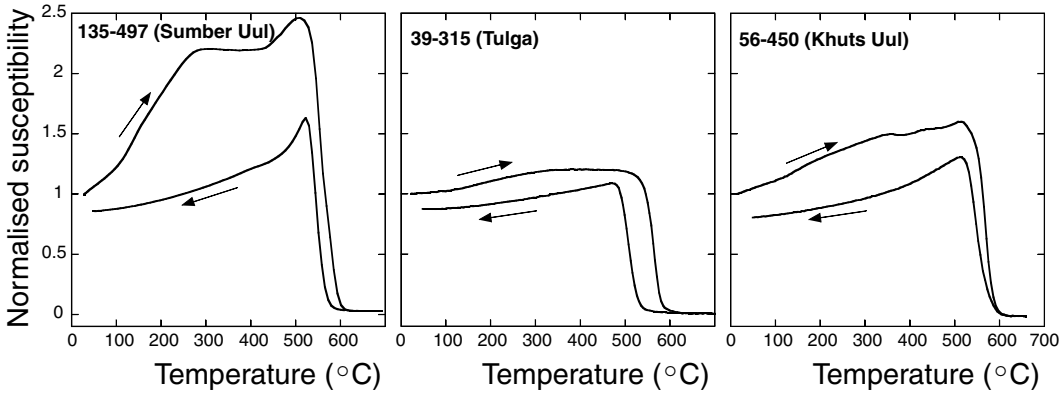

Figure 3. Thermomagnetic curves of magnetic susceptibility of representative specimens from the Sumber Uul, Tulga and Khuts Uul basaltic lava flows. Magnetic susceptibility has been normalized to the initial room temperature magnetic susceptibility. Arrows indicate heating and cooling parts of the cycle.

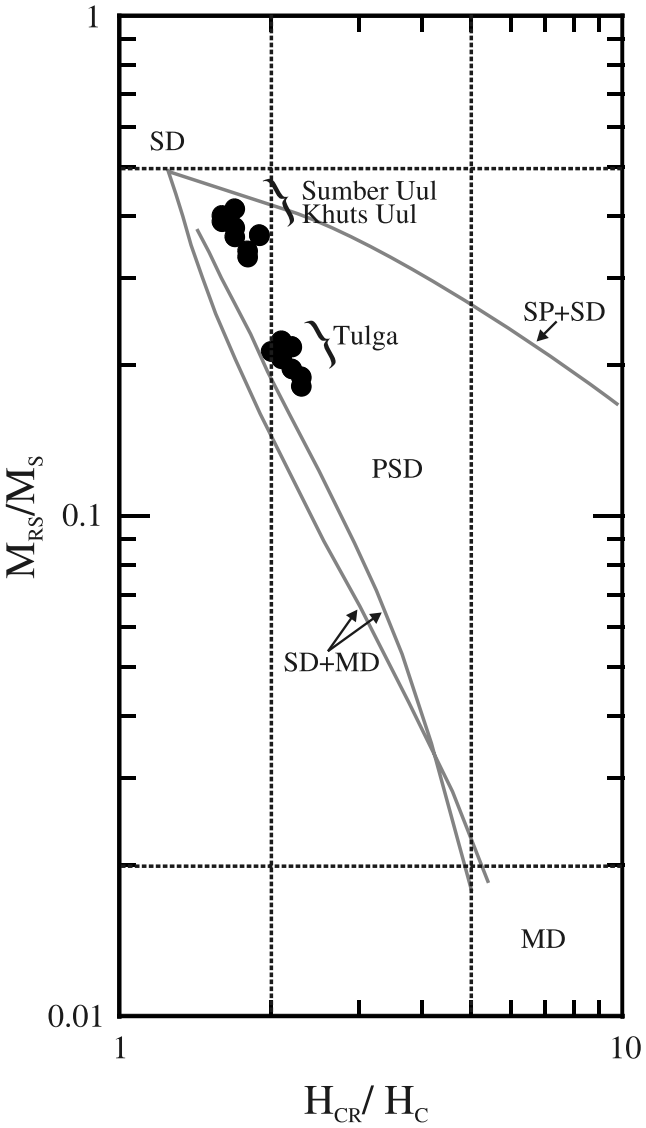

Figure 4. Day *et al.* (1977) plot showing that the measured specimens cluster in two mean grain sizes: Sumber Uul and Khuts Uul specimens plot very near the theoretical uniaxial single domain (SD) magnetite particle, lying in between the SD + multidomain (MD) and SD + superparamagnetic (SP) mixing curves of Dunlop (2002; grey curves). Tulga specimens show slightly coarser mean magnetic grain size falling on the SD + MD mixing curve.

stable characteristic component A between 250 and 580–600 °C or in peak fields between 6 and 100 mT. However, for certain specimens, component B was poorly separated from component A, leading to a great-circle path of points (Fig. 5b). For these specimens, we followed the remagnetization great-circle technique to resolve the characteristic component A. Site-mean directions of sites 131, 132 and 136–139 (Table 2) were, therefore, computed using the combined average of vectors and great-circle of McFadden & McElhinny (1988).

Thermal demagnetization curves, at Sumber Uul as well as at Tulga and Khuts Uul, more often than not reveal two drops in NRM intensity associated with component A. (Note that the remanence associated to the viscous component B unblocked by 200 °C represents less than 5 per cent of the total NRM). The first drop is at ∼400 °C and the other is associated with magnetite's unblocking temperature near 580 °C (for example, see Fig. 5a). As mentioned above, the palaeomagnetic vector orientation remains unchanged throughout the 200–600 °C temperature range. The decrease in NRM between 200 and 400 °C observed for example in sample 135–497 in Fig. 5(a) coincides with the broad maximum observed in thermomagnetic susceptibility curves (see Fig. 3) which we attributed in Section 4.2 to the heating induced inversion of maghemite to hematite. The drop in NRM intensity between 200 and 400 °C would, therefore, be carried by maghemite, formed from the low temperature oxidation of primary magnetite. Its remanence is, therefore, a secondary chemical remanent magnetization (CRM) but because of the nearly identical lattice parameters of magnetite and maghemite exchange coupling is expected to persist across the phase boundary resulting in the CRM orientation being parallel to the primary TRM orientation carried by magnetite (see p. 374 in Dunlop & Özdemir 1997). Consequently the use of the full temperature range covering the CRM and TRM to compute the characteristic remanent magnetization (ChRM) direction is justified in the limit that both define the same direction.

The combined site-mean directions of component A and great circles from the Sumber Uul locality are illustrated in Fig. 6 (dots) and listed in Table 2. Because of underlying horizontal redbeds, we do not apply any tilt correction to these directions. Moreover, according to our field observations, site 137 displays an anomalous tectonic setting which we were not able to resolve, whereas other flows appear flat-lying. This flow-mean direction (site 137, Fig. 6) has, therefore, been excluded from the final mean computation, as it is clearly an outlier. We note that all flow mean directions are of reverse polarity, with south upwards inclinations (Fig. 6), consistent

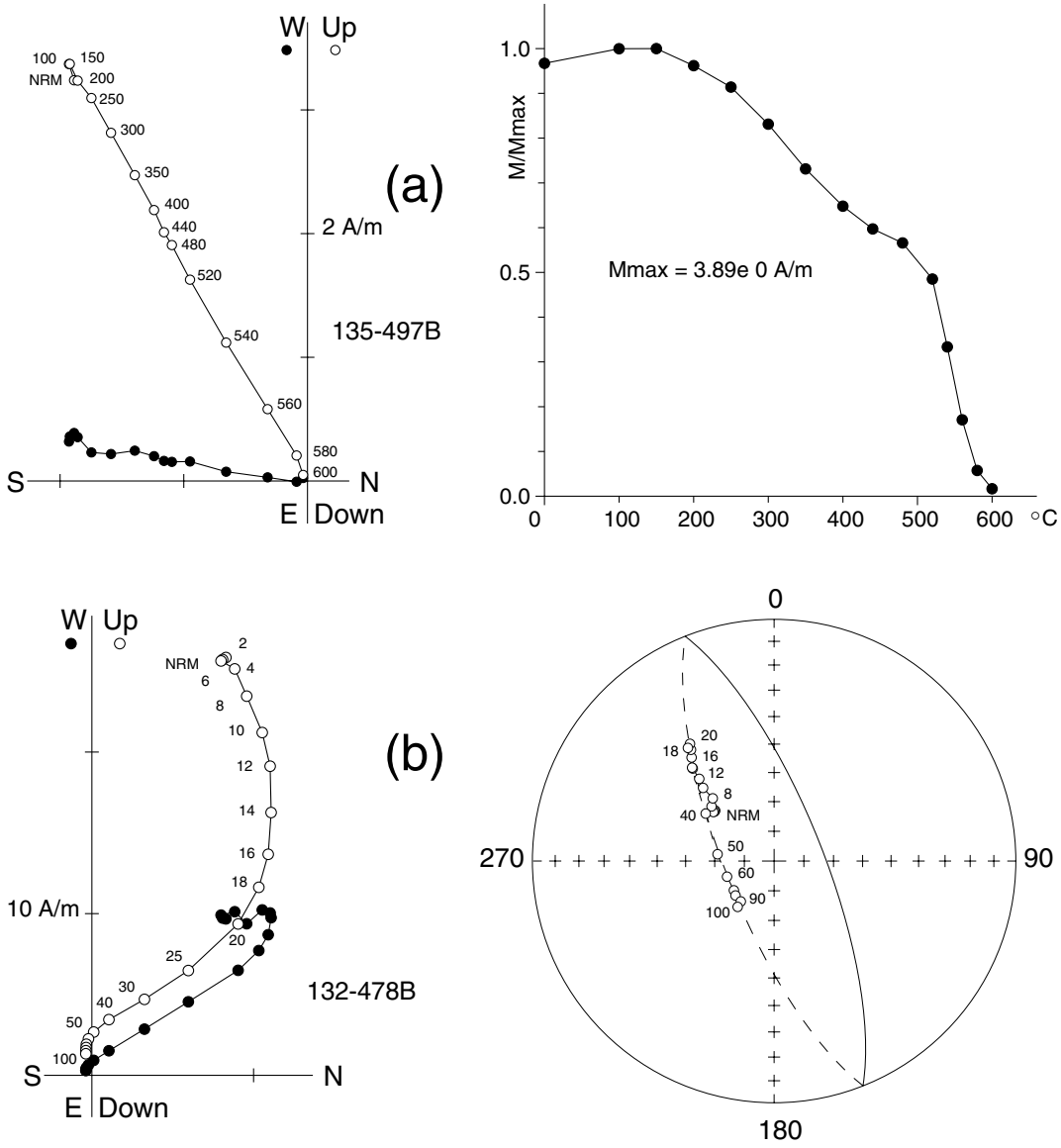

Figure 5. Orthogonal projections of magnetization vector end points during thermal and alternating field (AF) demagnetization experiments for Sumber Uul (62.2 Ma) specimens; (a) (left-hand side): orthogonal vector plot (Zijderveld 1967) of thermal demagnetization exhibiting a single magnetic component; temperatures are given in °C; (right-hand side): magnetization intensity decay curve; (b) (left-hand side): orthogonal vector plot showing overlapping unblocking spectra between two magnetization components; in that case, data are interpreted using the remagnetization great-circle method, shown on the stereonet to the right-hand side; AF steps are given in mT; black (white) symbols in orthogonal vector plots in (a) and (b) projection onto the horizontal (vertical) plane; black (white) symbols in stereonet in (b) downward (upward) pointing vectors.

with the reverse magnetic field during chron C27R in the Early Palaeocene (Danian; Cande & Kent 1995; Gradstein *et al.* 2004). The Sumber Uul locality average palaeomagnetic direction ($D = 181.9°$, $I = -64.2°$, $k = 252.9$, $\alpha_{95} = 3.2°$, $n = 9$; Table 2) lies very close to the present-day dipole and IGRF field directions, in reverse polarity. However, because all flow mean directions are reverse, and magnetization is carried by stable SD to nearly SD magnetite, we assume we have recovered the 62.2 Ma palaeomagnetic field for this area.

4.3.2 Tulga

In this region, 53 cores were collected from seven sites. Each site represents one discrete flow. NRM intensities of the basalt samples also fall into two distinct groups. In the first group (sites 35, 36, and 39–41), NRM ranges from 1.7 to 11.0 A m^{-1} with a mean value at 4.4 ± 2.1 A m^{-1} ($n = 33$). The second group (sites 37 and 38) exhibits anomalously higher values, ranging from 11 to 64 A m^{-1}, with a mean value at 29.9 ± 27.5 A m^{-1} (n = 16). We suspect lightning to have isothermally magnetized these specimens.

Representative orthogonal vector plots of two specimens shown in Figs 7(a) and (b) illustrate the general behaviour of most samples. Principal component analysis allowed separation of a single dominant component A in most specimens (sites 35, 38, 40 and 41). Similarly to specimens from Sumber Uul, component A is generally resolved at 590 °C temperature (Fig. 7a) after removing a B-component of either viscous or weathering origin unblocking at about 200 °C. Such is not the case for all

Table 2. Site-mean palaeomagnetic direction for component A of effusive rocks from Sumber Uul and Tulga regions.

Id/flow	Type	*n*/*N*	*Dg* (°)	*Ig* (°)	*k*	α_{95} (°)
Sumber Uul (42.6°N, 104.0°E) – 62.2 ± 0.9 Ma						
131	2 ht + 3 gc	5/6	199.3	−65.5	199.8	6.2
132	1 ht + 4 gc	5/6	176.8	−64.6	143.0	6.7
133	ht	8/8	179.6	−62.5	393.8	2.8
134	ht	5/8	171.6	−65.1	133.5	6.6
135	ht	8/8	185.0	−62.3	110.0	5.3
136	5 ht + 3 gc	8/8	175.0	−65.7	384.5	2.9
137[a]	6 ht + 2 gc	8/8	302.8	−50.9	49.1	8.0
138	6 ht + 3 gc	9/9	170.7	−58.8	36.3	8.7
139	2 ht + 6 gc	8/9	188.8	−68.0	441.1	2.4
140	ht	9/9	192.6	−62.3	343.1	2.8
Mean Sumber Uul		9/10	181.9	-64.2	252.9	3.2
Tulga (43.2°N, 104.1°E) – 62.0±5.0 Ma						
35	ht	7/7	148.3	−68.9	994.1	1.9
36	5 ht + 2 gc	6/7	181.0	−63.1	237.3	4.6
37[a]	4 ht + 3 gc	7/7	88.8	−28.2	350.6	3.6
38[a]	ht	6/6	15.5	−20.8	86.6	7.2
39	3 ht + 5 gc	5/8	161.0	−68.7	372.0	4.3
40	ht	6/6	175.4	−62.1	180.7	5.1
41	ht	6/7	190.4	−67.1	473.0	3.1
Mean Tulga		5/7	172.2	−66.6	126.6	6.8
Mean Sumber Uul-Tulga		14/17	358.7	65.1	175.4	3.0

ht and gc: number of HTC and remagnetization great-circles entering the statistics; *n*/*N*: number of samples used in the statistics/number of demagnetized specimens; *Dg*/*Ig* (*Ds*/*Is*): declination/inclination in geographic coordinates, *in situ* (stratigraphic coordinates, after tilt-correction); *k*, α_{95}: parameters of Fisher Statistics.
[a]Sites or flows excluded from the final mean calculation.

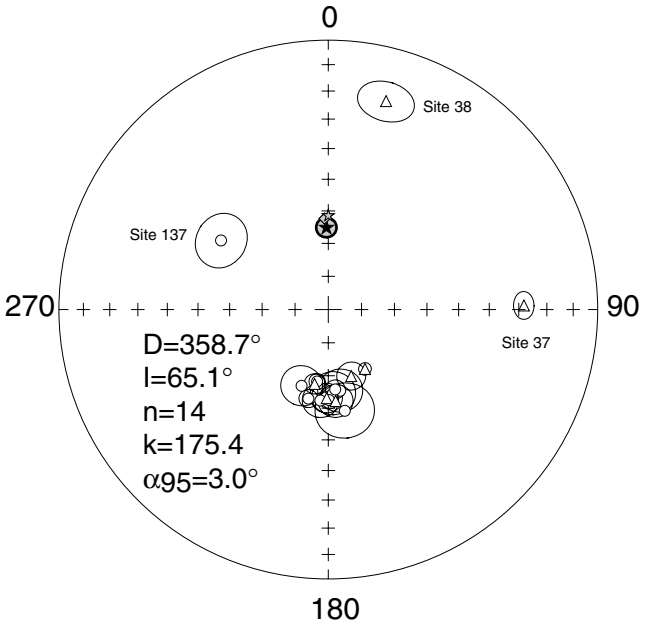

Figure 6. Equal-area projection of Sumber Uul (dots) and Tulga (triangles) site-mean directions of component A in geographic coordinates, with their α_{95} circles of confidence; black star with shaded α_{95} area: overall-mean direction in normal polarity; outlier sites 37, 38 and 137 are excluded from the final mean direction calculation; solid (open) symbols: positive, downward (negative, upward) inclinations; grey diamond (star): International Geomagnetic Reference Field (Dipolar Field) direction.

samples from sites 36, 37 and 39, where magnetization vector end points align on great-circle trajectories because component A and B's unblocking temperature spectra overlap (Fig. 7b). For this reason, the site-mean directions from these sites have been computed using the combined average direction of McFadden & McElhinny (1988).

Site-mean directions of component A from the Tulga locality are illustrated as triangles in Fig. 6, where they display a single reverse polarity. Sites 37 and 38 exhibit anomalous directions, which could be linked to their high NRM intensities. This reinforces the idea that lightning might have isothermally remagnetized these sites. Although data cluster upon a tilt correction (ks/kg = 140.4/126.6), we observed in the field that local dips are probably original and, therefore, are not linked to tectonics. Moreover, the underlying sediments that outcrop locally have horizontal bedding surfaces. Therefore, we assume that no bedding correction is required for this locality and that directions in geographic coordinates most likely represent the geomagnetic field direction at the time of flow emplacement during the chron C27R (Cande & Kent 1995; Gradstein *et al.* 2004). The average palaeomagnetic direction of the five basalt flows is $D = 172.2°$; $I = -66.6°$ ($n = 5/7$ flows; $k = 126.6$; $\alpha_{95} = 6.8°$).

4.3.3 Combined Sumber Uul-Tulga mean palaeomagnetic direction

In order to increase the number of flows of ∼62 Ma age, we propose to combine directions from the Sumber Uul locality (nine lava flows) with those from Tulga region (five lava flows), because of (1) their similar ages (62.1 ± 0.9 versus 62.0 ± 5.0 Ma) and (2) their geographic proximity, Sumber Uul being at 42.6°N/104.0°E and Tulga at 43.2°N/104.1°E, (representing a distance of ∼70 km). Fig. 6 shows site-mean directions from Sumber Uul (dots) and those from Tulga (triangles). Populations are not statistically different from one another. Thus, we have recomputed individual *in situ* flow-mean directions of Tulga at Sumber Uul location (Table 2). As discussed above, site-mean directions from sites 37 and 38 from Tulga and 137 from Sumber Uul appear as outliers and have been excluded from

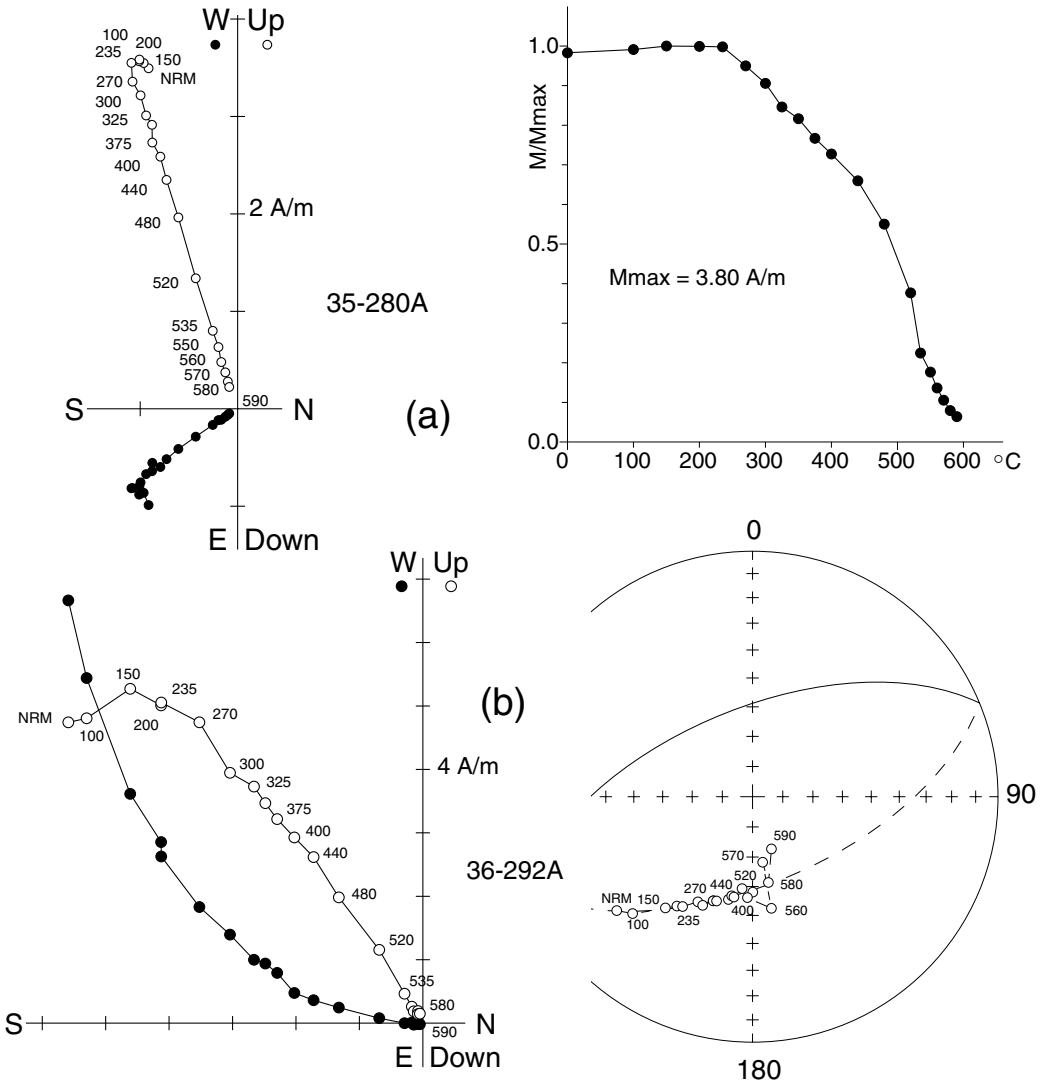

Figure 7. Orthogonal projections of magnetization vector end points during thermal demagnetization experiments for Tulga (62 Ma) specimens; (a) orthogonal vector plot (Zijderveld 1967) of thermal demagnetization exhibiting a single magnetic component, after removal of a low-temperature component by 200 °C (left-hand side) and magnetization decay curve (right-hand side); temperatures are given in °C; (b) orthogonal projection of thermal demagnetization of a sample showing two partly overlapping components of magnetization (left-hand side) and corresponding evolution along a great-circle (right-hand side). Same conventions, symbols and indications used as in Fig. 5.

the final mean computation. The combined final average palaeomagnetic direction for these 14 Early Palaeocene flows from Sumber Uul and Tulga (in normal polarity, Fig. 6) is: $D_m = 358.7^\circ$, $I_m = 65.1^\circ$ ($n = 14/17$ flows, $k = 175.4$, $\alpha_{95} = 3.0^\circ$). Because of assumed flat-lying flows and the lack of normal polarity results, we have no stability test to ascertain the primary origin of magnetization, and the final mean direction in normal polarity is very close to both Present day dipole and IGRF directions (Fig. 6). However, based on the rock magnetic analyses, component A is carried by stable SD to nearly SD magnetite, and all the data are of reverse polarity, excluding the possibility of a present-day remagnetization. We therefore, assume that we have recovered the 62.1 ± 5.9 Ma field direction in this region.

4.3.4 Khuts Uul region

In this locality, 114 samples were subjected to stepwise thermal demagnetization up to a maximum temperature of 620 °C. NRM intensity averages 6.9 ± 4.3 A m^{-1} ($n = 114$). Typical examples of thermal demagnetization illustrating the general behaviour of samples are shown in orthogonal vector plots of Figs 8(a) and (b). These orthogonal diagrams show that the demagnetization path trends linearly towards the origin defining a single A-component between 250 and 590–600 °C. Component A is resolved after removal of a weak viscous B-component unblocking by 200–250 °C. Component A site-mean directions are listed in Table 3 and illustrated in equal-area projections (Fig. 9), before (left-hand side) and after (right-hand side) tilt-correction. Directions exhibit a single reverse polarity consistent with the reverse magnetic field during chron C25R in the Early Palaeocene (Thanetian; Cande & Kent 1995; Gradstein *et al.* 2004), and they cluster upon unfolding. The site-mean direction of site 49 lies away from the others (∼20° from the final average direction) after tilt-correction. This may be due to either erroneous measurement of the flow attitude in the field or a locally rotated site. Therefore, this site has been excluded from the final mean direction computation. Although flow tilts are generally weak, the precision

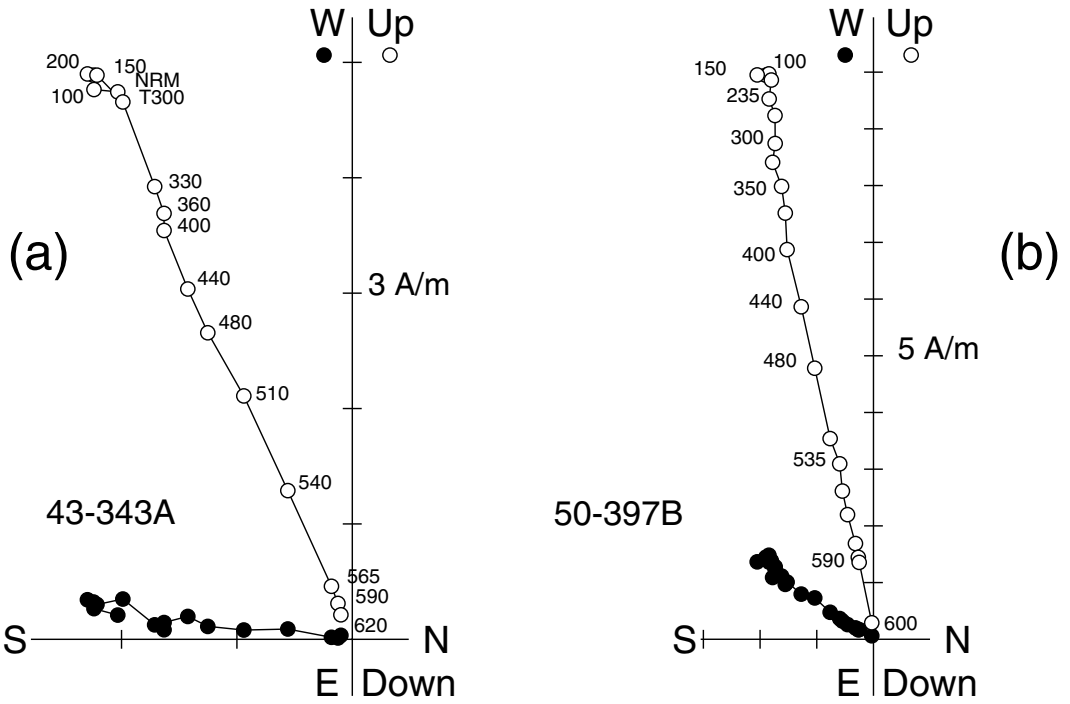

Figure 8. Orthogonal projections of magnetization vector end points during thermal demagnetization experiments for Khuts Uul (57.1 Ma) specimens; orthogonal vector plots (Zijderveld 1967) of representative specimens from (a) southern and (b) northern parts of the canyon at the Khuts Uul locality exhibiting a single magnetic component. Same conventions, symbols and indications used as in Fig. 5.

Table 3. Site-mean A-component directions of effusive rocks from Khuts Uul region (43.2°N, 104.6°E) −57.1 ± 0.8 Ma.

Id/flow	Strike/dip (°)	*n*/*N*	*Dg* (°)	*Ig* (°)	*Ds* (°)	*Is* (°)	*k*	α_{95} (°)
42	335.0/8.0	7/7	187.5	−77.4	208.9	−71.9	347.4	3.2
43	335.0/8.0	5/5	191.8	−62.1	201.9	−56.8	194.4	5.5
44	335.0/8.0	6/6	182.1	−85.0	221.4	−78.8	257.3	4.2
45–47	Flat lying	21/22	180.4	−83.8	180.4	−83.8	598.1	1.3
48	270.0/24.0	7/7	98.9	−83.5	165.1	−64.2	137.1	5.2
49[a]	254.0/17.0	3/3	190.4	−54.2	183.4	−38.5	776.6	4.4
50–51	Flat lying	13/13	205.0	−73.5	205.0	−73.5	534.2	1.8
52		6/6	201.2	−69.5	201.2	−69.5	218.9	4.5
53		6/6	209.5	−72.1	209.5	−72.1	174.1	5.1
54		5/5	216.4	−71.2	216.4	−71.2	246.1	4.9
55		7/7	199.3	−70.6	199.3	−70.6	311.8	3.4
56		7/7	211.1	−64.1	211.1	−64.1	83.0	6.7
57		7/7	209.7	−69.4	209.7	−69.4	843.8	2.1
58	332.0/15.0	6/6	221.6	−84.6	236.5	−69.8	518.3	2.9
59	332.0/15.0	7/7	206.5	−70.7	206.5	−70.7	104.4	5.9
Mean Khuts Uul		14/15	201.5	−74.9	–	–	78.7	4.5
			–	–	205.2	−71.2	92.0	4.2

Id/flow: site or flow names; strike/dip of flows; *n*/*N*: number of samples used in the statistics/number of demagnetized specimens; *Dg*/*Ig* (*Ds*/*Is*): declination/inclination in geographic coordinates, *in situ* (stratigraphic coordinates, after tilt-correction); *k*, α_{95}: parameters of Fisher Statistics.

[a]Flow 49 excluded from the final mean.

parameter *k* (Fisher 1953) increases from 78.7 to 92.0, leading to a positive fold test at 95 per cent level of confidence (McFadden 1990). This appears consistent with the north and northeast weak tilts of the underlying volcanoclastic sediments, as observed in the field. Therefore, we conclude that component A in tilt-corrected coordinates is likely the primary magnetization for these 14 basaltic lava flows. The average palaeomagnetic direction for the Khuts Uul locality is Ds = 205.2°, I = −71.2° (n = 14, k = 92.0, α_{95} = 4.2°).

5 DISCUSSION

Thermal and AF demagnetization of specimens from the basalt flows we sampled in the Sumber Uul, Tulga and Khuts Uul localities revealed a stable magnetization carried by SD to nearly SD magnetite, which we interpret as the primary magnetization. A secondary CRM carried by maghemite as a result of low temperature oxidation of magnetite is defined by an orientation paralleling the primary magnetization carried by magnetite due to exchange coupling persisting

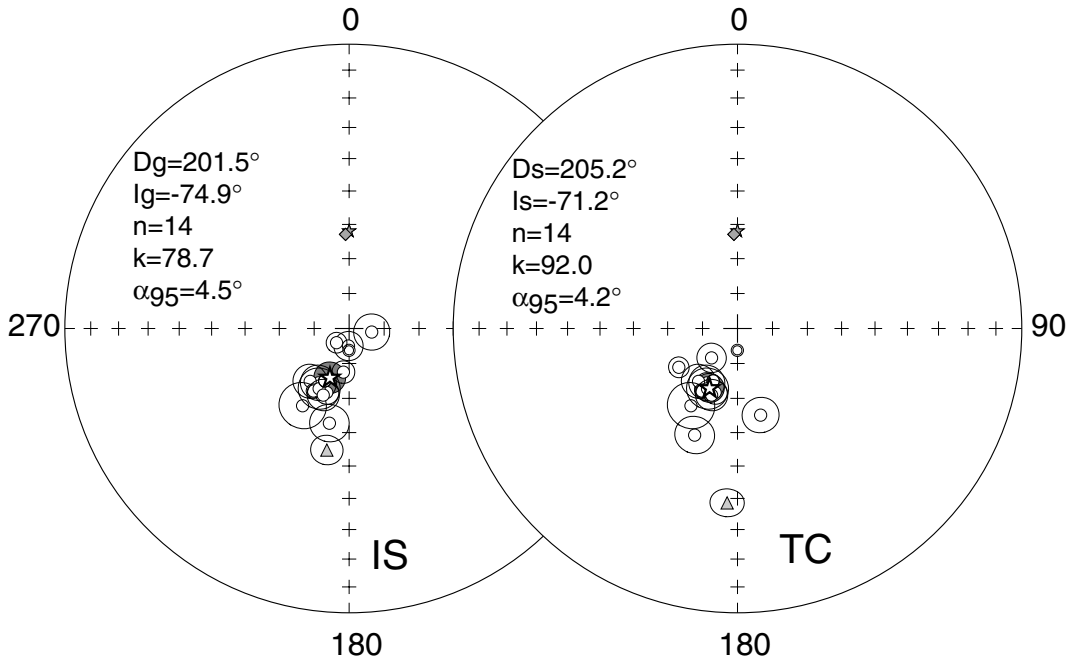

Figure 9. Equal-area projections of Khuts Uul site-mean directions of component A, with their α_{95} circles of confidence before (left-hand side) and after (right-hand side) tilt-correction; white stars with shaded α_{95} area: overall-mean direction; grey triangle: site 49 excluded from the computation of the final mean; grey diamond (star): International Geomagnetic Reference Field (Dipolar Field) direction. Same conventions used as in Fig. 6.

Table 4. Selected Early Palaeocene palaeomagnetic poles from Asia and reference APWP poles for Europe.

Name	Age	Slat	Slon	Plat	Plon	d*p*/d*m* or A_{95}	References
Europe APWP	60			81.1	190.5	2.9	Besse & Courtillot (2002)
APWP[a]	63.5			78.2	161.5	3.6	After Moreau *et al.* (2007)
APWP[a]	59.1			74.3	151.5	2.2	After Moreau *et al.* (2007)
Toru-Aygyr	55	42.6	76.4	75.0	220.9	8.7/13.2	Thomas *et al.* (1993)
Khuts Uul	57.1±0.8	43.2	104.6	69.6	148.0	6.3/7.3	This study
Tuoyun	59.5±2.6	40.2	75.3	49.0	160.9	7.9	Huang *et al.* (2005)
Sumber Uul-Tulga	62.1±5.9	42.6	104.0	85.2	92.5	3.9/4.9	This study
Sikhote Alin	66	44.0	135.0	85.8	347.1	12.7/16.8	Otofuji *et al.* (1995)

Slat, Slon (Plat, Plon): latitude and longitude of sites (palaeopoles); d*p*/d*m*: half-angles of ellipse of confidence; A_{95}: radius of 95 per cent cone of confidence.
[a]Reference poles at 63.5 and 59.1 Ma after the master APWP in Stable Africa coordinates of Moreau *et al.* (2007), transferred onto Eurasia using rotation parameters of Besse & Courtillot (2002).

across the maghemite/magnetite phase boundaries. This parallelism justifies the use of the combined CRM and TRM temperature ranges in computing the primary magnetization direction. Because of identical ages and proximity of outcrops, we combined the 14 flow mean palaeomagnetic directions from Sumber Uul (62.2 ± 0.9 Ma; this study) and Tulga (62.0 ± 5.0 Ma; Yarmolyuk *et al.* 1995) localities to compute a palaeopole which lies at $\lambda = 85.2°$N, $\phi = 92.5°$E, d*p*/d*m* = 3.9/4.9 (average age: 62.1 ± 5.9 Ma, Table 4, white diamond with light grey d*p*/d*m* area of confidence in Fig. 10a). Data from the Khuts Uul yield a palaeopole of $\lambda = 69.6°$N, $\phi = 148.0°$E, d*p*/d*m* = 6.3/7.3 (average age: 57.1 ± 0.8 Ma), computed after the tilt-corrected mean directions obtained on 14 basaltic lava flows from 18 sites (Table 4, white square with dark grey d*p*/d*m* area of confidence in Fig. 10a). At first sight, these two poles differ from one another, and also from the 60 Ma pole from the European reference APWP (Besse & Courtillot 2002).

Albeit very close, the d*p*/d*m* ellipse of confidence of Sumber Uul-Tulga palaeopole (Fig. 10a) does not contain either the present day north pole, or the 60 Ma pole from the European reference APWP (Besse & Courtillot 2002). The angular distance between the latter and our 62 Ma Sumber Uul-Tulga palaeopole amounts to 10.7° ± 4.9°, which may be decomposed into a component of counter-clockwise local rotation of the locality of Rot = −13.5° ± 7.0°, likely due to post-India/Asia collision tectonics, and a marginally significant palaeolatitude difference of $\Delta\lambda = -4.8° \pm 3.9°$. As underlined by the differences between small-circles passing through Sumber Uul-Tulga palaeopole (continuous black line in Fig. 10a) and the 60 Ma reference pole (black dotted line), our 62 Ma pole displays a slightly near-sided position with respect to the reference pole and the site location. Accordingly, the palaeomagnetic inclinations at sites are steeper than the expected ones by 3.8° ± 3.1.

Concerning our 57 Ma Khuts Uul palaeopole, it also occupies a near-sided position with respect to the European APWP 60 Ma reference pole (Table 4, Fig. 10a). The angular distance between them amounts to 15.0° ± 6.9° which translates into a marginally

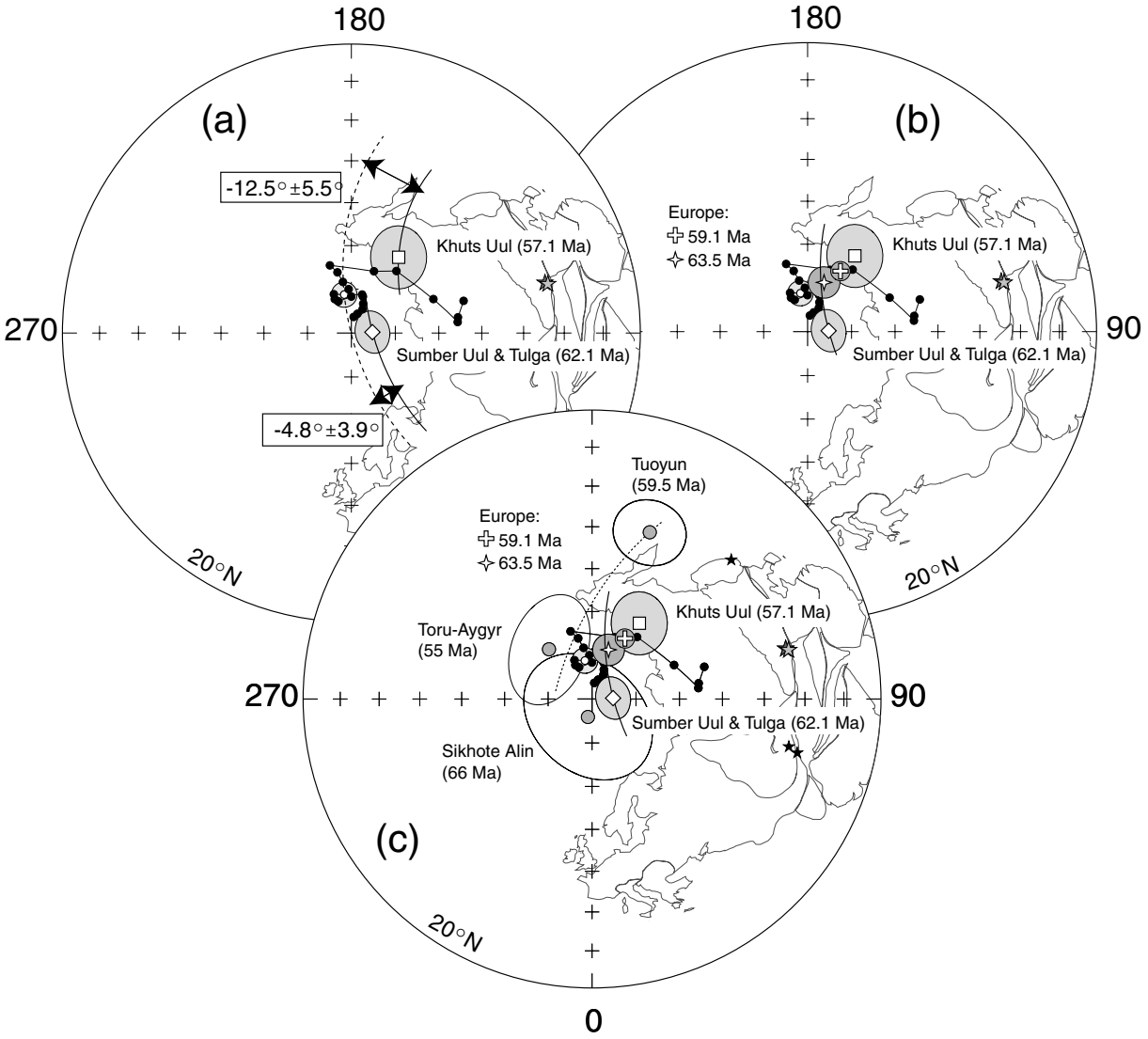

Figure 10. Equal-area projections of the Earth's northern hemisphere limited to the 20°N latitude; (a), (b) and (c): white diamond (square) with light grey d*p*/d*m* ellipse of confidence: Sumber Uul-Tulga (Khuts-Uul) palaeopole; stars: sites location; small linked solid dots: reference APWP poles for Europe (Bessa & Courtillot 2002); white dot with light grey A95 circle of confidence: 60 Ma European APWP reference pole; (a) dotted line: small-circle running through the 60 Ma reference pole centred on our site locations; solid lines: small-circles passing through Sumber Uul-Tulga and Khuts Uul poles, and centred on the average site locations; (b) white plus and 4-branches star: 59.1 and 63.5 Ma (median age) poles after Moreau *et al.* (2007) synthetic APWP poles for 65.5-61.6 Ma (chrons 29-27) and 61.6-56.7 Ma (chrons 26-25) periods, respectively, with their A95 circles of confidence; solid line: small-circle passing through Sumber Uul-Tulga palaeopole; (c) grey dots: coeval palaeopoles from Sikhote Alin in eastern Russia, Tuoyun in the Tarim basin and Toru Aygyr in the Tien Shan; light dotted line: small-circle centred on Tuoyun locality and passing through the palaeopole; solid line as in (b); stars: sites location.

significant local clockwise rotation of the Khuts Uul locality around a vertical axis of Rot $= 12.9 \pm 11.9°$, but a large and near-sided location of the Khuts Uul palaeopole of $\Delta\lambda = -12.5 \pm 5.5°$, with respect to the reference pole. The near-sided location of the palaeopole results from a palaeomagnetic inclination which is $9.2° \pm 4.1°$ steeper than expected based on the European APWP 60 Ma reference pole. Several hypotheses can be advocated to explain these anomalous positions of Sumber Uul-Tulga and Khuts Uul poles, but none of them are satisfying. (1) An error in the estimated age of these basalts; in effect, our Khuts Uul pole is fully consistent with the 160 Ma reference pole of European APWP. However, volcanic activity in the region has been dated as ranging from ∼50 to 73 Ma by Yarmolyuk *et al.* (1995), and our own K-Ar age determination using the Cassignol–Gillot technique (Cassignol & Gillot 1982) results in a well-constrained ages of 57.1 ± 0.8 and 62.1 ± 5.9 Ma for Khuts Uul and Sumber Uul-Tulga effusive rocks. We therefore, exclude the hypothesis of a Middle Jurassic age of this formation. (2) A tectonic hypothesis; this is inconceivable as well, because Cretaceous palaeopoles from Siberia and Amuria (Pruner 1992; Cogné *et al.* 2005; Hankard *et al.* 2007b) are consistent with the 100–120 Ma part of the European APWP, and the Eocene palaeomagnetic data from Amuria (Hankard *et al.* 2007a) reveal that Amuria (and probably Siberia) were located ∼1500 km more to the south than expected, because of anomalously shallow inclinations. Interpreted as purely due to north–south relative movements between Siberia and Amuria, our Khuts Uul pole would suggest the unacceptable scenario of a ∼1350 km northward convergence of Amuria with respect to Siberia between the Cretaceous and the Palaeocene,

followed by a ∼2850 km of divergence (i.e. extension) between the Palaeocene and the Eocene, ending up with a ∼1500 km northward convergence between the Eocene and present. Indeed, this scenario completely contradicts our knowledge of Asian tectonics in this period. (3) A long-lasting non-dipolar field in the Tertiary; this hypothesis, which has been advocated to explain anomalous inclinations in Tertiary formations from Central Asia (e.g. Kent & Smethurst 1998; Si & Van der Voo 2001; Torsvik *et al.* 2001), would imply a shallowing of palaeomagnetic inclinations at mid-latitudes, whereas the abnormal position of Khuts Uul palaeopole (and to a lesser extent that of Sumber Uul-Tulga pole) results from anomalously steep inclinations. We therefore, exclude this third hypothesis.

There is however a fourth and more convincing scenario. While our poles do not conform to the European APWP poles, they appear to be fully consistent with the new high-resolution synthetic APWP for the 65–42 Ma period established by Moreau *et al.* (2007) (Fig. 10b). Their synthetic APWP is calculated by stacking six magnetostratigraphic sequences, three from sedimentary basins in Europe (Gubbio in Italy, Aix-en-Provence in France, and Basque basin in Spain) and three others from ODP legs (leg 74 on the Africa plate, 121 from Australia and 171B from North America). The authors highlight a loop in the synthetic APWP with, in particular, a cusp at anomalies 26–25 (61–56 Ma), which differs from the European APWP of Besse & Courtillot (2002). Because of worldwide similarities between magnetostratigraphies, the authors argue for an episode of true polar wander (TPW) as the origin of this loop, which they constrain with climatic data from near-polar regions. We have transferred this APWP onto Europe, using the global kinematic parameters of Besse & Courtillot (2002; Fig. 10b). Our 62.2 ± 5.9 Ma Sumber Uul-Tulga and 57.1 ± 0.8 Ma Khuts Uul poles are coherent with Moreau *et al.* (2007) reference poles for 65.5–61.6 Ma (defined between chrons 29 and 27; median age: 63.5 Ma) and 61.6–56.7 Ma (defined between chrons 26 and 25; median age: 59.1 Ma) ages, respectively (Fig. 10b).

The angular distance between Khuts Uul and the 59.1 Ma poles results in both insignificant relative rotation of 6.2° ± 13.5°, and relative palaeolatitude displacement of $\Delta\lambda = -3.2° \pm 6.1°$. Therefore, we propose that the anomalous near-sided position of Khuts Uul palaeopole results from this newly evidenced TPW episode in the Palaeocene. Similarly, Sumber Uul-Tulga palaeopole does not display either any significant palaeolatitude offset ($\Delta\lambda = 0.7° \pm 4.9°$) with respect to the 63.5 Ma APWP pole. However, it exhibits a small but significant counter-clockwise rotation of $R = -16.4° \pm 9.0°$ of the studied area around a vertical axis, as evidenced by the small-circle centred on Sumber Uul locality (black line in Fig. 10b) passing through the palaeopole and the reference 63.5 Ma pole of Moreau *et al.* (2007). Although we have no detailed fault maps, and accounting for Cenozoic tectonic activity within the Amuria block (e.g. Cunningham 1996, 1997), such small Cenozoic or more recent local rotations are not uncommon (e.g. see Hankard *et al.* 2007a). Overall, taking into account this TPW episode, we suggest that Palaeocene palaeopoles from Mongolia (and Siberia) are consistent with European ones. We thus conclude that, for the Cretaceous (e.g. Hankard *et al.* 2007b), European APWP (including this TPW episode) properly describes eastern parts of the continent until at least the Early Palaeocene.

As a final point, we compare our data to previously published coeval poles from Central Asia (grey dots in Fig. 10c). Only three early Palaeocene palaeopoles can be found in the literature: a 66.0 Ma pole from Sikhote Alin welded tuffs (Otofuji *et al.* 1995), a 59.5 Ma pole obtained by Huang *et al.* (2005) on 14 basaltic lava flows from Tuoyun locality in Tarim basin, and a 55.0 Ma pole obtained by Thomas *et al.* (1993) on 4 basaltic flows at Toru Aygyr in Kazakhstan. The 66.0 Ma Sikhote Alin pole appears to conform to our 62.1 Ma palaeopole from Sumber Uul-Tulga (Fig. 10c), mainly due to the large d*p*/d*m* ellipse of confidence of the former. In contrast, both 55.0 and 59.5 Ma poles (neglecting the large clockwise rotation of the latter) appear far-sided with respect to our 57.1 Ma Khuts Uul pole, by 15.8 ± 8.6° and 11.5 ± 8.1°, respectively. Beyond the small number of points defining the Toru Aygyr 55.0 Ma pole, this discrepancy could arise from the superimposition of two mechanisms or causes. First, the age difference between these poles (55, 57.1 and 59.5 Ma) is critical during the fast TPW episode proposed by Moreau *et al.* (2007). In effect, the rapid oscillations of the Geocentric Axial Dipole (GAD) evidenced by this APWP mainly result in apparent palaeolatitude variations as viewed from Asia. A second cause might reside in the fact that both Toru Aygyr and Tuoyun areas are located just north of the northwestern tip of India indentor, further west than our Mongolian localities. Therefore, a part of the far-sided position of these two poles could actually result from a relative palaeolatitudinal change between western and eastern zones, with western parts of the system having suffered a northward movement with respect to both Siberia and Amuria after the Palaeocene. Unfortunately, the amount of such relative movements is impossible to define more precisely, because of the age problem just discussed, but we suggest that it could be of the order of several hundred of kilometres (more than ∼380 km, the lowest limit of the far-sided position at the 95 per cent confidence level, as quoted above). This interpretation is in conflict with the interpretation of Huang *et al.* (2005), but we underline that this most probably arises from the lack of accuracy of the 50–60 Ma part of the reference APWP (Besse & Courtillot 2002), as demonstrated by Moreau *et al.* (2007).

6 CONCLUSION

We have presented new palaeomagnetic results obtained at three volcanic localities (Sumber Uul, Tulga and Khuts Uul) of Early Palaeocene age located in the Gobi Desert of Mongolia. Our own K-Ar dating of these formations allowed to precise the age of Sumber Uul (62.2 ± 0.9 Ma) and Khuts Uul (57.1 ± 0.8 Ma) localities. From Khuts Uul and combined Sumber Uul-Tulga (62.1 ± 5.9 Ma) palaeomagnetic results, we propose two new palaeomagnetic poles for the Amuria block of Central Asia.

The interpretation of these poles is not straightforward. The combined Sumber Uul-Tulga 62.1 Ma pole appears fairly consistent with the 60 Ma reference APWP pole for Europe (Besse & Courtillot 2002). In contrast, the 57.1 Ma Khuts Uul palaeopole appears largely near-sided with respect to the 60 Ma reference pole from the European APWP and site location. However, our poles are fully consistent with the new high-resolution synthetic APWP for the 65–42 Ma period of Moreau *et al.* (2007). This APWP, which is correlated with climatic data, exhibits a cusp between chrons 26 and 25 (61.6–56.7 Ma) resulting from an episode of TPW which is not characterized in the European APWP of Besse & Courtillot (2002). We conclude that our new Palaeocene poles from the Amuria block (and probably Siberia, because of the lack of north–south relative movements between the two since the Palaeocene) are not significantly different from European palaeopoles, providing this TPW is taken into account.

This has two major consequences. (1) Our results are in line with the admitted conclusions that Amuria block, North China Block (NCB), South China Block (SCB) and Siberia apparently form a rigid tectonic unit since the Late Jurassic–Early Cretaceous, and that this assemblage did not undergo any relative latitudinal motion since that time (Zhao & Coe 1987; Zhao *et al.* 1990; Enkin *et al.* 1992; Ma *et al.* 1993a,b; Gilder *et al.* 1996a; Gilder & Courtillot 1997; Halim *et al.* 1998a, b; Yang & Besse 2001; Yang *et al.* 2001; Kravchinsky *et al.* 2002; Cogné *et al.* 2005, Hankard *et al.* 2007b). (2) The second conclusion concerns the Tertiary Inclination Shallowing Anomaly in Central Asia. Our studies, as well as previously published ones, of Cretaceous effusive formations from Siberia and Amuria (Zhao *et al.* 1990; Pruner 1992; Cogné *et al.* 2005; Hankard *et al.* 2007b) indeed showed a consistency between palaeomagnetic poles from these regions, and poles from the synthetic APWP for Europe. In contrast, palaeomagnetic studies of either effusive or sedimentary Eocene and later formations (Thomas *et al.* 1993, 1994; Westphal 1993; Chauvin *et al.* 1996; Gilder *et al.* 1996b, 2001, 2003; Cogné *et al.* 1999; Dupont-Nivet *et al.* 2002; Huang *et al.* 2004; Yan *et al.* 2006; Hankard *et al.* 2007a) all revealed anomalously shallow inclinations. We have recently proposed (Hankard *et al.* 2007a) that this anomaly amounts to $8.0^\circ \pm 4.7^\circ$ in effusive rocks from Khaton Sudal in Mongolia, dated at 39.4 ± 0.6 Ma. From the results of the present study of Palaeocene palaeopoles we conclude that the anomaly of Central Asia palaeomagnetic inclinations in effusive rocks begins after ∼60 Ma and before ∼40 Ma. Only further palaeomagnetic studies of Early Eocene effusive formations from Central Asia could help define better time constraints on the onset of the shallowing inclination anomaly.

ACKNOWLEDGMENTS

We wish to thank O. Tamurtogoo, G. Badarch and J. Badamgarav from the Geological Institute of Mongolian Academy of Sciences, for efficient organization and guiding in the field during 1999 expedition to Gobi desert. This study is part of cooperation between IPGP and The Mongolian University of Science and Technology. We thank Uyanga, Khatna and Moogii for their efficient help during the 2004 field expedition. A. Hildenbrand and J.C. Lefèvre kindly assisted F.H. for K-Ar dating of Sumber Uul and Khuts Uul samples. K. Kodama and Y. Otofuji provided helpful and constructive criticisms of an early draft of this paper. This is contribution 2272 of IPGP.

REFERENCES

Besse, J. & Courtillot, V., 2002. Apparent and true polar wander and the geometry of the geomagnetic field over the last 200 Myrs, *J. geophys. Res.,* **107,** 1–31.

Cande, S.C. & Kent, D.V., 1995. Revised calibration of the geomagnetic polarity timescale for the Late Cretaceous and Cenozoic, *J. geophys. Res.,* **100,** 6093–6095.

Cassignol, C. & Gillot, P.-Y., 1982. Range and effectiveness of unspiked potassium-argon dating, in *Numerical Dating in Stratigraphy,* pp. 159–172, ed. O. edit, Wiley, Chichester.

Chauvin, A., Perroud, H. & Bazhenov, M.L., 1996. Anomalous low paleomagnetic inclinations from Oligocene-Lower Miocene red beds of southwest Tien Shan, Central Asia, *Geophys. J. Int.,* **126,** 303–313.

Chen, Y., Cogné, J.P., Courtillot, V., Tapponnier, P. & Zhu, X.Y., 1993a. Cretaceous paleomagnetic results from western Tibet and tectonic implications, *J. geophys. Res.,* **98,** 17 981–17 999.

Chen, Y., Courtillot, V., Cogné, J.-P., Besse, J., Yang, Z. & Enkin, R., 1993b. The configuration of Asia prior to the collision of India: Cretaceous paleomagnetic constraints, *J. geophys. Res.,* **98,** 21 927–21 941.

Cogné, J.P., 2003. PaleoMac: a Macintosh™ application for treating paleomagnetic data and making plate reconstructions, *Geochem. Geophys. Geosyst.,* **4,** 1007, doi:10.1029/2001GC000227.

Cogné, J.P., Halim, N., Chen, Y. & Courtillot, V., 1999. Resolving the problem of shallow magnetizations of Tertiary age in Asia: insights from paleomagnetic data from the Qiangtang, Kunlun, and Qaidam blocks (Tibet, China), and a new hypothesis, *J. geophys. Res.,* **104,** 17 715–17 734.

Cogné, J.P., Kravchinsky, V.A., Halim, N. & Hankard, F., 2005. Late Jurassic-Early Cretaceous closure of the Mongol-Okhotsk Ocean demonstrated by new Mesozoic paleomagnetic results from the Trans-Baïkal area (SE Siberia), *Geophys. J. Int.,* **163,** 813–832.

Cunningham, W.D., Windley, B.F., Dorjnamjaa, D., Badamgarov, J. & Saandar, M., 1996. Late Cenozoic transpression in southwestern Mongolia and the Gobi Altai-Tien Shan connection, *Earth planet. Sci. Lett.,* **140,** 67–81.

Cunningham, W.D., Windley, B.F., Owen, L.A., Barry, T., Dorjnamjaa, D. & Badamgarov, J., 1997. Geometry and style of partitioned deformation within a late Cenozoic transpressional zone in the eastern Gobi Altai Mountains, Mongolia, *Tectonophysics,* **277,** 285–306.

Day, R., Fuller, M. & Schmidt, V.A., 1977. Hysteresis properties of titanomagnetites: grain-size and compositional dependence, *Phys. Earth planet. Inter.,* **13,** 260–267.

Dunlop, D. J., 2002. Theory and application of the Day plot (Mrs/Ms versus Hcr/Hc) 1. Theoretical curves and tests using titanomagnetite data, *J. geophys. Res.,* **107,** 22.

Dunlop, D.J. & Özdemir, Ö. 1997. *Rock Magnetism: Fundamentals and Frontiers,* pp.1–573 Cambridge University Press, New York.

Dupont-Nivet, G., Guo, Z., Butler, R.F. & Jia, C., 2002. Discordant paleomagnetic direction in Miocene rocks from the central Tarim Basin: evidence for local deformation and inclination shallowing, *Earth planet. Sci. Lett.,* **199,** 473–482.

Enkin, R.J., Yang, Z., Chen, Y. & Courtillot, V., 1992. Paleomagnetic constraints on the geodynamic history of the major blocks of China from the permian to the present, *J. geophys. Res.,* **97,** 13 953–13 989.

Fisher, R.A., 1953. Dispersion on a sphere, *Proc. R. Soc. London, A,* **217,** 295–305.

Gilder, S.A. & Courtillot, V., 1997. Timing of North-South China collision from new middle to Late Mesozoic paleomagnetic data from the North China Block, *J. geophys. Res.,* **102,** 17 713–17 727.

Gilder, S.A., Coe, R.S., Wu, H., Kuang, G., Zhao, X., Wu, Q. & Tang, X., 1993. Cretaceous and tertiary paleomagnetic results from southeast China and their tectonic implications, *Earth planet. Sci. Lett.,* **117,** 637–652.

Gilder, S.A. *et al.*, 1996a. Isotopic and paleomagnetic constraints on the Mesozoic tectonic evolution of south China, *J. geophys. Res.,* **101,** 16 137–16 154.

Gilder, S.A., Zhao, X., Coe, R.S., Meng, Z., Courtillot, V. & Besse, J., 1996b. Paleomagnetism and tectonics of the Southern Tarim Basin, northwestern China, *J. geophys. Res.,* **101,** 22 015–22 031.

Gilder, S.A., Chen, Y. & Sen, S., 2001. Oligo-Miocene magnetostratigraphy and rock magnetism of the Xishuigou section, Subei (Gansu province, western China) and implications for shallow inclinations in central Asia, *J. geophys. Res.,* **106,** 30 505–30 521.

Gilder, S.A., Chen, Y., Cogné, J.-P., Tan, X., Courtillot, V., Sun, D. & Li, Y., 2003. Paleomagnetism of Upper Jurassic to Lower Cretaceous volcanic and sedimentary rocks from the western Tarim Basin and implications for inclination shallowing and absolute dating of the M-O (ISEA?) chron, *Earth planet. Sci. Lett.,* **206,** 587–600.

Gillot, P.-Y. & Cornette, Y., 1986. The Cassignol technique for potassium-argon dating, precision and accuracy: examples from the late Pleistocene to recent volcanics from southern Italy, *Chem. Geol. (Isotope Geoscience section),* **59,** 205–222.

Gradstein, F.M., Ogg, J.G., Smith, A.G. & 36 others, 2004. *A Geologic Time Scale 2004*. pp. 589, Cambridge University Press, Cambridge.

Grommé, C.S., Wright, T.L. & Peck, D.L., 1969. Magnetic properties and oxidation of iron-titanium oxide minerals in Alae and Makaopuhi lava lakes, Hawaii, *J. geophys. Res.,* **74**(22), 5277–5293.

Halim, N., Kravchinsky, V., Gilder, S., Cogné, J.P., Alexyutin, M., Sorokin, A., Courtillot, V. & Chen, Y., 1998a. A paleomagnetic study from the

Mongol-Okhotsk region: rotated Early Cretaceous volcanics and remagnetized sediments, *Earth planet. Sci. Lett.,* **159,** 133–145.

Halim, N. *et al.*, 1998b. New Cretaceous and Early Tertiary paleomagnetic results from Xining-Lanzhou basin, Kunlun and Qiangtang blocks, China: implications on the geodynamic evolution of Asia, *J. geophys. Res.,* **103**(B9), 21 025–21 045.

Halls, H.C., 1978. The use of converging remagnetization circles in paleomagnetism, *Phys. Earth Planet. Inter.,* **16,** 1–11.

Hankard, F., Cogné, J.P., Kravchinsky, V.A., Bayasgalan, A., Lklagvadorj, P. & Carporzen, L., 2007a. New Tertiary paleomagnetic poles from Mongolia and Siberia at 40, 30, 20 and 13 Ma: clues on the inclination shallowing problem in Central Asia, *J. geophys. Res.,* **112,** B02101, doi:10.1029/2006JB004488.

Hankard, F., Cogné, J.P., Quidelleur, X., Bayasgalan, A., Lklagvadorj, P. & Kravchinsky, V.A., 2007b. Paleomagnetism and K-Ar dating of Cretaceous basalts from Mongolia, *Geophys. J. Int.,* **169,** 898–908, doi:10.1111/j.1365-246X.2007.03292.x.

Huang, K. & Opdyke, N.D., 1992. Paleomagnetism of Cretaceous to Lower Tertiary rocks from Southwestern Sichuan: a revisit, *Earth planet. Sci. Lett.,* **112,** 29–40.

Huang, B.C., Wang, Y.C., Liu, T., Yang, T.S., Li, Y.A., Sun, D.J. & Zhu, R.X., 2004. Paleomagnetism of Miocene sediments from the Turfan Basin, Northwest China: no significant vertical-axis rotation during Neotectonic compression within the Tian Shan Range, Central Asia, *Tectonophysics,* **384,** 1–21.

Huang, B.C., Piper, J.D.A., Wang, Y., He, H. & Zhu, R., 2005. Paleomagnetic and geochronological constraints on the post-collisional northward convergence of the southwest Tian Shan, NW China, *Tectonophysics,* **409,** 107–124.

Huang, B.C., He, H.Y., Zhang, C.X. & Zhu, R.X., 2006. Paleomagnetic and geochronological study of the Halaqiaola basalts, southern margin of the Altai Mountains, northern Xinjiang: constraints on neotectonic convergent patterns north of Tibet, *J. geophys. Res.,* **111,** Art. No. B01101.

Kent, D.V. & Smethurst, M.A., 1998. Shallow bias of paleomagnetic inclinations in the Paleozoic and Precambrian, *Earth planet. Sci. Lett.,* **160**(3–4), 391–402.

Kirshvink, J.L., 1980. The least-squares line and plane and the analysis of palaeomagnetic data, *Geophys. J. R. astron. Soc.,* **62,** 699–718.

Kovalenko, D.V., Yarmolyuk, V.V. & Solov'ev, A.V., 1997. Migration of volcanic centers of the south Khangai hot spot: paleomagnetic evidence, *Geotectonics,* **31,** 228–235.

Kravchinsky, V.A., Cogné, J.P., Harbert, W. & Kuzmin, M.I., 2002. Evolution of the Mongol–Okhotsk Ocean as constrained by new palaeomagnetic data from the Mongol–Okhotsk suture zone, Siberia, *Geophys. J. Int.,* **148,** 34–57.

Liu, Z.F., Zhao, X.X., Wang, C.S., Liu, S. & Yi, H.S., 2003. Magnetostratigraphy of Tertiary sediments from the Hoh Xil Basin: implications for the Cenozoic tectonic history of the Tibetan Plateau, *Geophys. J. Int.,* **154,** 233–252.

Ma, X., Yang, Z. & Xing, L., 1993. The lower cretaceous reference pole for north China, and its tectonic implications, *Geophys. J. Int.,* **115,** 323–331.

McFadden, P.L., 1990. A new fold test for paleomagnetic studies, *Geophys. J. Int.,* **103,** 163–169.

McFadden, P.L. & McElhinny, M.W., 1988. The combined analysis of remagnetization circles and direct observations in paleomagnetism, *Earth planet. Sci. Lett.,* **87,** 161–172.

McFadden, P.L., Merill, R.T., McElhinny, M.W. & Sunhee, L., 1991. Reversal of the Earth's magnetic field and temporal variations of the dynamo families, *J. geophys. Res.,* **96,** 3923–3933.

Molnar, P. & Tapponnier, P., 1975. Cenozoic tectonics of Asia: effects of a continental collision, *Science,* **189,** 419–426.

Moreau, M.-G., Besse, J. & Fluteau, F., 2007. A new global Paleocene-Eocene apparent polar wandering path loop by "stacking" magnetostratigraphies: correlations with high latitude climatic data, *Earth planet. Sci. Lett.,* doi:10.1016/j.epsl.2007.05.025.

Narumoto, K., Yang, Z.Y., Takemoto, K., Zaman, H., Morinaga, H. & Otofuji, Y., 2006. Anomalously shallow inclination in middle-northernn part of the South China block: palaeomagnetic study of Late Cretaceous red beds from Yichang area, *Geophys. J. Int.,* **164,** 290–300.

Odin, G.S. *et al.*, 1982. Interlaboratory standards for dating purposes, in *Numerical Dating in Stratigraphy,* eds G.S. Odin., pp. 123–150, Wiley, Chichester.

Otofuji, Y. *et al.*, 1995. Late Cretaceous to early Paleogene paleomagnetic results from Sikhote Alin, far eastern Russia: implications for deformation of East Asia, *Earth planet. Sci. Lett.,* **130,** 95–108.

Patriat, P. & Achache, J., 1984. India-Eurasia collision chronology has implications for crustal shortening and driving mechanism of plates, *Nature,* **311,** 615–621.

Pruner, P., 1992. Paleomagnetism and paleogeography of Mongolia from the Carboniferous to Cretaceous – final report, *Phys. Earth planet. Inter.,* **70,** 169–177.

Quidelleur, X., Gillot, P.Y., Soler, V. & Lefèvre, J.C., 2001. K-Ar dating extended into the last millennium: application to youngest effusive episode of the Teide volcano (Spain), *Geophys. Res. Lett.,* **28,** 3067–3070.

Shuvalov, V.F. & Nikolaeva, T.V., 1985. On the age and spatial distribution of Cenozoic basalts in the south of Mongolia, *Vestnik LGU,* **14,** 52–59 (in Russian).

Si, J. & Van Der Voo, R., 2001. Too-low magnetic inclinaisons in central Asia: an indication of long-term Tertiary non-dipole field?, *Terra Nova,* **13,** 471–478.

Steiger, R.H. & Jaeger, E., 1977. Subcommission on geochronology: convention on the use of decay constants in geo- and cosmochronology, *Earth planet. Sci. Lett.,* **36,** 359–362.

Sun, Z.M., Yang, Z.Y., Pei, J.L., Yang, T.S. & Wang, X.S., 2006a. New Early Cretaceous paleomagnetic data from volcanic and red beds of the eastern Qaidam Block and its implications for tectonics of Central Asia, *Earth planet. Sci. Lett.,* **243,** 268–281.

Sun, Z.M., Yang, Z.Y., Yang, T.S., Pei, J.L. & Yu, Q.F., 2006b. New Late Cretaceous and Paleogene paleomagnetic results from south China and their geodynamic implications, *J. geophys. Res.,* **111,** Art. No. B03101.

Tan, X., Kodama, K.P., Chen, H., Fang, D., Sun, D. & Li, Y., 2003. Paleomagnetism and magnetic anisotropy of Cretaceous red beds from the Tarim basin, northwest China: evidence for a rock magnetic cause of anomalously shallow paleomagnetic inclinations from central Asia, *J. geophys. Res.,* **108,** 1–20.

Tapponnier, P. & Molnar, P., 1979. Active faulting and cenozoic tectonics of Tien Shan, Mongolia, and Baykal regions, *J. geophys. Res.,* **84,** 3425–3459.

Tauxe, L., 2005. Inclination flattening and the geocentric axial dipole hypothesis, *Earth planet. Sci. Lett.,* **233,** 247–261.

Thomas, J.C., Perroud, H., Cobbold, P.R., Bazhenov, M.L., Burtman, V.S., Chauvin, A. & Sadybokasof, E., 1993. A paleomagnetic study of Tertiary formations from the Kirgiz Tien Shan and its tectonic implications, *J. geophys. Res.,* **98,** 9571–9589.

Thomas, J.C., Chauvin, A., Gapais, D., Bazhenov, M.L., Perroud, H., Cobbold, P.R. & Burtman, V.S., 1994. Paleomagnetic evidence for Cenozoic block rotations in the Tadjik depression (Central Asia), *J. geophys. Res.,* **99,** 15 141–15 160.

Torsvik, T.H., Van Der Voo, R., Meert, J.G., Mosar, J. & Walderhaug, H.J., 2001. Reconstructions of the continents around the North Atlantic at about the 60th parallel, *Earth planet. Sci. Lett.,* **187,** 55–69.

Van Der Voo, R. & Torsvik, T.H., 2001. Evidence for late Paleozoic and Mesozoic non-dipole fields provides an explanation for the Pangea reconstruction problems, *Earth planet. Sci. Lett.,* **187,** 71–81.

Westphal, M., 1993. Did a large departure from the geocentric axial dipole occur during the Eocene? Evidence from the magnetic polar wander path of Eurasia, *Earth planet. Sci. Lett.,* **117,** 15–28.

Yan, M.D., Van Der Voo, R., Tauxe, L., Fang, X.M. & Parés, J.M., 2005. Shallow bias in Neogene palaeomagnetic directions from the Guide Basin, NE Tibet, caused by inclination error, *Geophys. J. Int.,* **163,** 944–948.

Yan, M.D., Van Der Voo, R., Fang, X.-M., Parés, J.M. & Rea, D.K., 2006. Paleomagnetic evidence for a mid-Miocene clockwise rotation of about 25° of the Guide Basin area in NE Tibet, *Earth planet. Sci. Lett.,* **241,** 234–247.

Yang, Z. & Besse, J., 1993. Paleomagnetic study of Permian and mesozoic sedimentary rocks from Northern Thailand supports the extrusion model for Indochina, *Earth planet. Sci. Lett.,* **117,** 525–552.

Yang, Z. & Besse, J., 2001. New Mesozoic apparent polar wander path for south China: tectonic consequences, *J. geophys. Res.,* **106,** 8493–8520.

Yang, Z., Yin, J., Otofuji, Y.I. & Sato, K., 2001. Discrepant Cretaceous paleomagnetic poles between Eastern China and Indochina: a consequence of the extrusion of Indochina, *Tectonophysics,* **334,** 101–113.

Yarmolyuk, V.V., Ivanov, V.G., Samoylov, V.S. & Arakelyants, M.M., 1995. Formation stages of Mesosoic and Cenozoic intraplate volcanism of South Mongolia, *Dokl. Acad. Nauk.,* **344**(5), 673–676 (In Russian).

Zhao, X. & Coe, R.S., 1987. Paleomagnetic constraints on the collision and rotation of North and South China, *Nature,* **327,** 141–144.

Zhao, X., Coe, R.S., Zhou, Y., Wu, H. & Wang, J., 1990. New paleomagnetic results from northern China: collision and suturing with Siberia and Kazakstan, *Tectonophysics,* **181**(43–81).

Zijderveld, J.D.A., 1967. A.C. demagnetization of rocks: analysis of results, in *Methods in Paleomagnetism,* pp. 254–286, eds D.W. Collinson, K.M. Creer and S.K. Runcorn, Elsevier, New York.